Automatic detection of the belt-like region in an image with variational PDE model

Shoutao Li (李寿涛)[1,2], Xiaomao Li (李小毛)[1,2], and Yandong Tang (唐延东)[1]

[1] *Shenyang Institute of Automation, Chinese Academy of Sciences, Shenyang 110016*
[2] *Graduate School of the Chinese Academy of Sciences, Beijing 100039*

Received December 12, 2006

In this paper, we propose a novel method to automatically detect the belt-like object, such as highway, river, etc., in a given image based on Mumford-Shah function and the evolution of two phase curves. The method can automatically detect two curves that are the boundaries of the belt-like object. In fact, this is a partition problem and we model it as an energy minimization of a Mumford-Shah function based minimal partition problem like active contour model. With Eulerian formulation the partial differential equations (PDEs) of curve evolution are given and the two curves will stop on the desired boundary. The stop term does not depend on the gradient of the image and the initial curves can be anywhere in the image. We also give a numerical algorithm using finite differences and present various experimental results. Compared with other methods, our method can directly detect the boundaries of belt-like object as two continuous curves, even if the image is very noisy.

OCIS codes: 100.0100, 150.0150.

The automatic detection of a belt-like region in an image is important. Many important object features in natural scenes or tissues of human body, such as rivers or blood vessels, correspond to such regions. Several approaches, like edge collection[1], active contour methods[2,3], and so on, are widely applied in the object segmentation and recognition. Approaches based on edge detection have some drawbacks. In fact, up to date, the edge detection is most frequently used to extract thin-belt-like road, river or other objects[4,5]. Edge detection as the essential part of these algorithms is sensitive to noises in an image. Denoising and object enhancing of the noisy images, as image pre-processing in these approaches, are always necessary for the correct object detection. When the image edges are extracted based on image gray gradient, they contain not only the boundaries of the object to be detected but also the boundaries of the other objects. The belt-like object must be identified among the detected edges, which usually include pseudo-edges and much more other edges that do not belong to the object to be detected. Due to the noises and the complex texture, the belt-like object usually cannot be detected as a continuous edge. Therefore, the post-processing, such as mathematical morphology transforms[6] or curve approximation, is also needed for the connectivity of edges to form the whole boundary of the belt-like object to be detected.

In 2001, based on Mumford-Shah segmentation techniques[7] and the level set method, Chan and Vese[3] proposed the active contour model without edge, also called C-V model, that can detect contours both with[8] or without gradient. In addition, in that model the initial curve can be anywhere in an image. In the active contour model, the contour to be detected is usually supposed to be a closed curve, and with level set method it is represented as the zero level set of a function defined in higher dimensions. It overcomes the drawbacks of the classic active contour models (or snake models) that are based on edge-detector, dependent on initial curve location and sensitive to noise. Because the belt-like objects appear in an image as two open curves that are not intersected, with the C-V model some contours of other objects, especially some closed contours, are also detected. After contour detection it is also required to recognize that curve is the object boundary.

Based on Mumford-Shah model[7] and variational PDE model and inspired by C-V model, with two phase curves we proposed a novel method to automatically detect the boundaries of the belt-like object in a given image. The evolving curves are two open curves and do not need to be represented as the zero level set of a function defined in higher dimensions. It is a development of the technique used in Ref. [9]. The initial curves, which are usually chosen as two parallel straight lines, can be anywhere in the image and they evolve and stop on the boundaries of the belt-like object in an image, even for a noisy image. In this way the belt-like object can be very well detected and preserved. Compared with classic snake models[10], which can also be used in the detection of an open curve boundary with their initial curves being near the boundaries of the object in noisy image, our model is more robust against image noise and its initial curve can be anywhere.

The Mumford-Shah piecewise smooth segmentation is defined by[7]

$$\inf_{u,\Gamma} E_{\mathrm{MS}}[u,\Gamma|u_0] = \int_{\Omega} |u-u_0|^2 \mathrm{d}x + \mu \int_{\Omega\backslash\Gamma} |\nabla u|^2 \mathrm{d}x + \nu \cdot L(\Gamma), \quad (1)$$

where $u_0 : \overline{\Omega} \to \Re$ is a given image, μ and ν are the positive parameters. The solution image u obtained by minimizing this function is formed by smooth disjoint regions R_i and with their boundaries denoted by Γ, where $\bigcup_i R_i = \Omega\backslash\Gamma$. $L(\Gamma)$ represents the length of Γ. It allows

1671-7694/2007/050270-04

for segmenting an image into some disjoint homogenous regions with smoothly varying intensities and the boundaries with sharp varying intensities. This model has been used extensively in image segmentation, denoising, inpainting, and computer vision.

The detection of the belt-like object in a given image is the process of seeking two open curves running across this image that divide the image into three homogenous regions, as shown in Fig. 1.

The image is denoted as a rectangular region Ω: $(0,a)\times(0,b)$. The analytical equations of the curves positioned above and below are $y=\phi_1^0(x)$, $y=\phi_2^0(x)$, $0\le x\le a$, respectively.

The three regions separated by the two curves are

$$\begin{cases} R_{\text{above}(C_1^0)}=\{(x,y)\in\Omega: y>\varphi_1^0(x)\} \\ R_{\text{above}(C_2^0)\text{ and below}(C_1^0)}=\{(x,y)\in\Omega: \\ \qquad\qquad y>\varphi_2^0(x)\text{ and } y<\varphi_1^0(x)\} \\ R_{\text{below}(C_2^0)}=\{(x,y)\in\Omega: y<\varphi_2^0(x)\} \end{cases}, \tag{2}$$

where C_1^0 denotes the curve in the upper part of the image and C_2^0 is the lower one.

We assume that the image u_0 is made up of three regions of approximatively piecewise-constant intensities (see Fig. 2) and from above to below they have distinct values c_1^0, c_2^0, c_3^0.

Assume C_1 and C_2 denote the two curves above and below in the above image. The meanings of c_1, c_2, c_3 are similar to those of c_1^0, c_2^0, c_3^0.

Now we consider the fitting term

$$\begin{aligned}\text{Fit}(C_1,C_2)=&\int_{\text{above}(C_1)}|u_0(x,y)-c_1|^2\mathrm{d}x\mathrm{d}y\\&+\int_{\text{below}(C_2)}|u_0(x,y)-c_3|^2\mathrm{d}x\mathrm{d}y\\&+\int_{\text{above}(C_2)\text{ and below}(C_1)}|u_0(x,y)-c_2|^2\mathrm{d}x\mathrm{d}y.\end{aligned}\tag{3}$$

Fig. 1. Two white curves separate the image into three homogenous regions.

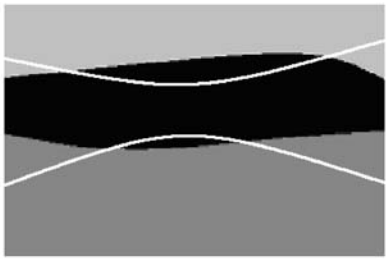

Fig. 2. Image with three parts and initial curves.

When $C_1=C_1^0$, $C_2=C_2^0$, Fit $=0$. So if we want to segment the image, we only need to minimize "Fit".

Equation (3) can be thought as a piecewise constant segmentation that is a particular case of the Mumford-Shah model and called the minimal partition problem.

Adding the length term into Eq. (3), we have the complete fitting term of our model:

$$\begin{aligned}\text{Fit}(c_1,c_2,c_3,C_1,C_2)=&\mu(L(C_1)+L(C_2))\\&+\lambda\Big(\int_{\text{above}(C_1)}|u_0(x,y)-c_1|^2\mathrm{d}x\mathrm{d}y\\&+\int_{\text{below}(C_2)}|u_0(x,y)-c_3|^2\mathrm{d}x\mathrm{d}y\\&+\int_{\text{above}(C_2)\text{ and below}(C_1)}|u_0(x,y)-c_2|^2\mathrm{d}x\mathrm{d}y\Big).\end{aligned}\tag{4}$$

Now using the Heaviside function $H(x)$, the one-dimensional (1D) Dirac measure $\delta(x)$ and the curve definition $y=\phi_1(x)$, $y=\phi_2(x)$, $0\le x\le a$, the fitting term, also called energy function, has the form as

$$\begin{aligned}\text{Fit}(c_1,c_2,c_3,C_1,C_2)=&\mu\Big(\int_{[0,a]}\sqrt{(1+(\frac{\mathrm{d}\varphi_1(x)}{\mathrm{d}x})^2)}\mathrm{d}x\\&+\int_{[0,a]}\sqrt{(1+(\frac{\mathrm{d}\varphi_2(x)}{\mathrm{d}x})^2)}\mathrm{d}x\Big)\\&+\lambda\int_\Omega|u_0(x,y)-c_1|^2H(y-\varphi_1(x))\mathrm{d}x\mathrm{d}y\\&+\lambda\int_\Omega|u_0(x,y)-c_3|^2(1-H(y-\varphi_2(x)))\mathrm{d}x\mathrm{d}y\\&+\lambda\int_\Omega|u_0(x,y)-c_2|^2(1-H(y-\varphi_1(x)))H(y-\varphi_2(x))\mathrm{d}x\mathrm{d}y,\end{aligned}\tag{5}$$

where

$$H(x)=\begin{cases}1, & \text{if } x\ge 0\\ 0, & \text{if } x<0\end{cases},\quad \delta(x)=\begin{cases}1, & \text{if } x=0\\ 0, & \text{if } x\ne 0\end{cases}.\tag{6}$$

The constants c_1, c_2, and c_3 are given by

$$c_1=\frac{\int_\Omega u_0H(y-\varphi_1)\mathrm{d}x\mathrm{d}y}{\int_\Omega H(y-\varphi_1)\mathrm{d}x\mathrm{d}y},$$

$$c_2=\frac{\int_\Omega u_0(1-H(y-\varphi_1))H(\varphi_2)\mathrm{d}x\mathrm{d}y}{\int_\Omega(1-H(y-\varphi_1))H(\varphi_2)\mathrm{d}x\mathrm{d}y},$$

$$c_3 = \frac{\int\limits_{\Omega} u_0(1 - H(y - \varphi_2))\mathrm{d}x\mathrm{d}y}{\int\limits_{\Omega} 1 - H(y - \varphi_2)\mathrm{d}x\mathrm{d}y}. \quad (7)$$

So our model can be written as the minimization problem $\inf\limits_{c_1,c_2,c_3,C_1,C_2} \mathrm{Fit}(c_1, c_2, c_3, C_1, C_2)$.

In order to compute the associated Euler-Lagrange equation, we adopt the regularized versions of the functions H and δ, as denoted by H_ε and δ_ε[3], and $\delta_\varepsilon(x) = \frac{\mathrm{d}H_\varepsilon(x)}{\mathrm{d}x}$.

Keeping c_1, c_2, c_3 fixed, we minimize $\mathrm{Fit}(c_1, c_2, c_3, C_1, C_2)$. The associated Euler-Lagrange equation for φ_1, φ_2 with parameterizing the descent direction by an artificial time $t >= 0$ is deduced.

The set of equations are

$$\frac{\partial\varphi_1(t,x)}{\partial t} = \mu\frac{\partial}{\partial x}\left(\frac{1}{\sqrt{1 + (\frac{\partial\varphi_1(t,x)}{\partial x})^2}}\left(\frac{\partial\varphi_1(t,x)}{\partial x}\right)\right)$$

$$+\lambda((u_0(x, \varphi_1(t,x)) - c_1)^2$$

$$-H(\varphi_1(t,x) - \varphi_2(t,x))(u_0(x, \varphi_1(t,x)) - c_2)^2), \quad (8)$$

$\frac{\partial\varphi_1(t,0)}{\partial x} = 0$ and $\frac{\partial\varphi_1(t,X_0)}{\partial x} = 0$ (the boundary conditions), $\varphi_1(0,x) = \psi_0(x)$ (the initial condition);

$$\frac{\partial\varphi_2(t,x)}{\partial t} = \mu\frac{\partial}{\partial x}\left(\frac{1}{\sqrt{1 + (\frac{\partial\varphi_2(t,x)}{\partial x})^2}}\left(\frac{\partial\varphi_2(t,x)}{\partial x}\right)\right)$$

$$+\lambda(H(\varphi_1(t,x) - \varphi_2(t,x))$$

$$+(u_0(x, \varphi_2(t,x)) - c_2)^2 - (u_0(x, \varphi_2(t,x)) - c_3)^2), \quad (9)$$

$\frac{\partial\varphi_2(t,0)}{\partial x} = 0$ and $\frac{\partial\varphi_2(t,X_0)}{\partial x} = 0$ (the boundary conditions), $\varphi_2(0,x) = \eta_0(x)$ (the initial condition).

Let the steady solution of Eqs. (8) and (9) be $\varphi_1(T,x)$ and $\varphi_2(T,x)$. Then the boundary curves of the belt-like region are $y = \varphi_1(T,x)$ and $y = \varphi_2(T,x)$.

In our experiments, we assume $\varphi_1 > \varphi_2$ so that the Heaviside function $H(x)$ can be eliminated from Eqs. (8) and (9). First we need to present some definitions: h, the space step; Δt, the time step; and $x_i = ih$ $(0 =< i <= a)$ being the points evenly distributed. Let $\phi_{1i}^n = \phi_1(n\Delta t, ih)$ be an approximation of $\phi_1(t,x)$ with $n > 0$. The finite differences of Eqs. (8) and (9) are denoted as

$$\Delta_-\varphi_\iota = \varphi_\iota - \varphi_{\iota-1}, \Delta_+ = \varphi_{\iota+1} - \varphi_\iota. \quad (10)$$

The dicretization of Eq. (8) is

$$\frac{\varphi_{1i}^{n+1} - \varphi_{1i}^n}{\Delta t} = \frac{\mu}{h^2}\Delta_-\left(\frac{\Delta_+\varphi_{1i}^n}{\sqrt{1 + (\frac{\Delta_+\varphi_{1i}^n}{h})^2}}\right)$$

$$+\lambda((U_0(ih, \varphi_{1i}^n) - c_1(\varphi_{1i}^n))^2 - (U_0(ih, \varphi_{1i}^n) - c_2(\varphi_{1i}^n))^2). \quad (11)$$

The discretization of Eq. (9) is similar to that of Eq. (8).

The initial curves can be anywhere. In our experiments, the y axis points downward. As to the other parameters, $h = 1$, $\Delta t = 0.03$, $\mu = 0.0004 \times 255 \times 255$, $\lambda = 0.0006 \times 255 \times 255$. Figure 3 shows the process of detecting the boundaries of the river in the grassland.

In the following figures the middle phase figures will not be displayed. The algorithm proposed here has been used in Fire Watch to segment the forest areas of an image (see Fig. 4). In Fig. 5, it is easy to understand the ability of the algorithm against noise. Figure 6 is a noised image with a river in it.

In this paper, we propose a new method which is useful to detect a belt-like region running through an image horizontally. It is effective and insensitive to noise. It

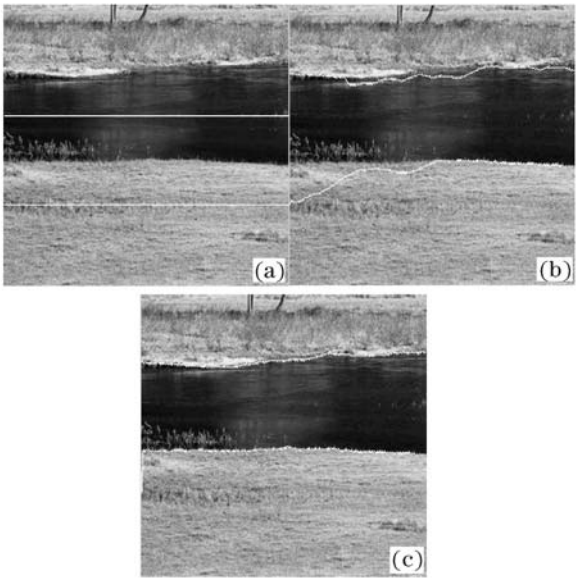

Fig. 3. (a) Original image; (b) evolving curve; (c) resulting image.

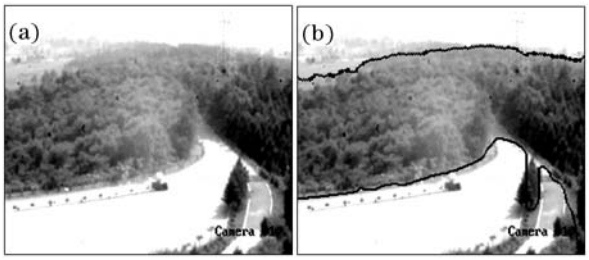

Fig. 4. (a) Original image and (b) segmented image.

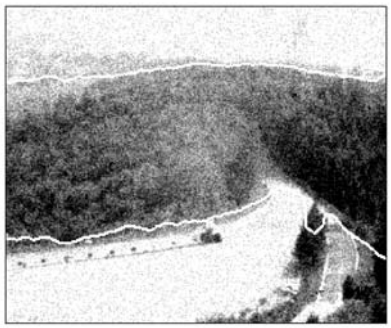

Fig. 5. Image polluted by noise and the detection result.

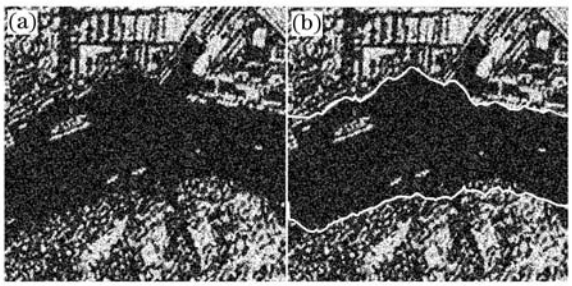

Fig. 6. (a) Noised image with a river in the middle and (b) the detection result.

also has some limitations and disadvantages. The time needed for processing is not satisfactory, slightly long in practice, especially when the intensity differences of the three parts of the image are small or the middle part is not broad enough.

Still much improvement is possible. For example, the curves we get in the experiments are those that can be represented by $y = \varphi(x)$. We hope the curves could be denoted in a more general form. The further result will be published in our future articles.

Y. Tang is the author to whom the correspondence should be addressed, his e-mail address is ytang@sia.cn.

References

1. C. Shao, K. Tang, Z. Yang, G. Cheng, and J. Kan, J. Optoelectronics·Laser (in Chinese) **15,** 985 (2004).
2. L. Min, Y. Tang, and Z. Shi, Infrared and Laser Engineering (in Chinese) **35,** 499 (2006).
3. T. F. Chan and L. A. Vese, IEEE Trans. Image Processing **10,** 266 (2001).
4. C. Jia and G. Kuang, Journal of Image and Graphics (in Chinese) **10,** 1218 (2005).
5. T. Wang and T. Jiang, Journal of Institute of Surveying and Mapping (in Chinese) **21,** 187 (2004).
6. J. Qu, C. Wang, and Z. Wang, in *Proceedings of International Geoscience and Remote Sensing Symposium* **6,** 3420 (2002).
7. D. Mumford and J. Shah, Commun. Pure Appl. Math. **42,** 577 (1989).
8. W. K. Law and A. C. S. Chung, in *Proceedings of the 2006 Conference on Computer Vision and Pattern Recognition Workshop* (2006).
9. Y. Tang, Y. Wang, and C. Eigenbrod, Chin. Opt. Lett. **4,** 460 (2006).
10. M. Kass, A. Witkin, and D. Terzopoulos, Int. J. Comput. Vis. **1,** 321 (1988).